

A Comprehensive Study of Reconfigurable Intelligent Surfaces in Generalized Fading

Imène Trigui, Member, *IEEE*, Wessam Ajib, Senior Member, *IEEE*, and Wei-Ping Zhu, Senior Member, *IEEE*.

Abstract—Leveraging on the reconfigurable intelligent surface (RIS) paradigm for enabling the next Internet of Things (IoT) and 6G era, this paper develops a comprehensive theoretical framework characterizing the performance of RIS-assisted communications in a plethora of propagation environments. We derive unified mathematical models for the outage probability and ergodic capacity of single and multiple-element RIS over Fox’s \mathcal{H} fading channel, which includes as special cases nearly all linear and non linear multi-path and shadowing fading models adopted in the open literature. For gleaning further insights, we capitalize on the algebraic asymptotic expansions of the \mathcal{H} -transform to further analyze the outage probability and capacity at high signal-to-noise ratio (SNR) in a unified fashion. Asymptotic analysis shows two scaling rates of the outage probability at large average SNR. Moreover, by harnessing its tractability, the developed statistical machinery is employed to characterize the performance of multiple randomly distributed RIS-assisted communications over Fox’s \mathcal{H} fading channels. We show that there is a great potential to improve the outage performance and thereby the capacity when fewer RISs are deployed each with more reflecting elements.

Index Terms—Reconfigurable intelligent surface (RIS), Fox’s \mathcal{H} -fading, channel capacity, path-loss model.

I. INTRODUCTION

Contemporary wireless networks modeling and analysis is a vibrant topic that keeps taking new dimensions in complexity as researchers relentlessly keep exploring the potential of novel breakthrough technologies to support upcoming Internet of Things (IoT) and 6G era [1]. Among these emerging technologies, reconfigurable intelligent surfaces (RISs) [2],[3], have been introduced with an overarching vision of artificially controlling the wireless environment as to increase the quality of service and spectrum efficiency. RIS is based on massive integration of low-cost tunable passive elements that will get weaved into conventional buildings and objects able to transmit data by reflecting and modulating an incident RF wave [3], which leads to a more controllable wireless environment. Leveraging in this key property, RIS-enabled networks challenge the deviceside approaches such as massive multiple-input-multiple-output (MIMO) systems, encoding, modulation, and relaying, currently deployed in wireless networks to fully adapt to the time-variant, unpredictable channel state. However, being fundamentally different, the RIS concept asks for new methods for modeling, analyzing, and optimizing RIS-enhanced wireless networks, yet this is still in its embryonic stage in the open literature. The so far valuable attempts to study RIS systems include [4]- [6] where several precoding optimality studies for RIS-assisted communications in terms of rate and energy efficiency have been achieved relying on

real-time RIS phases shift control. Recently, the interesting problems of joint active and passive beamforming and secrecy enhancement are investigated in [7] and [8], respectively. Even more recently, researchers focused on outage probability [9] and asymptotic data rate [10] analysis for RIS-based systems. Moreover, the authors of [2], [11] adopted an upper bound for the average symbol error probability (SEP) harnessing on the central limit theorem (CLT) when the number of reflecting elements grows large. Unfortunately, the available results, typically providing bounds and approximations, only consider Rayleigh fading distribution, thereby hindering the applicability of RIS-based model in setup scenarios that capture practical multi-path and shadowing conditions. Indeed, shadowing along with high attenuation are the main impairments at mmWave frequencies. While RIS communications are envisioned as powerful enabler for higher frequency communications, a careful characterization of RIS-assisted systems over composite fading conditions is crucial. Triggered by the above background, our work is pioneer in incorporating a comprehensive multiple-parameter fading model for general case multi-path and/or shadowing into tractable performance analysis for RIS-assisted systems without the use of CLT approximation. On the other hand, there is a lack of literature on the impact of the locations of multiple RISs. In [14], the authors investigate a single-cell multiuser system aided by multiple co-located intelligent surfaces (equivalent to a single large RIS). However, the different works in [2]- [14] consider either a single RIS or multiple RISs at given locations, and have not addressed the multi-RISs deployment issue, which is practically important for RIS-assisted wireless systems. In this study, using BPP to simulate the RIS’s locations, we develop the first comprehensive mathematical model accounting for spatial randomness of multiple RISs in generalized fading.

Our contributions can be summarized as follows:

- We propose a novel RIS framework, where Fox’s \mathcal{H} transform theory is invoked for modelling, in a unified fashion, any RIS-based fading environments in terms of closed-form outage probability and ergodic capacity.
- We draw multiple useful link-level insights from the proposed analysis. For instance, we show that the diversity gain scales with the number of elements per RIS multiplied by the worst distribution of the fading between the base station-RIS and RIS-user links.
- We study and analyze a wireless network with large-scale deployment of RISs. Under the nearest RIS association strategy, we derive the outage probability by averaging over random RIS/user distance and generalized fading.

- We evaluate the derived outage probability and ergodic capacity expressions by simulations, and investigate the effect of key system and fading parameters on RIS performance and large-scale deployment.

The rest of this paper is organized as follows. Section II describes the system model and the types of fading discussed in this paper. Then, Sections III is devoted to the unified performance analysis framework where the ergodic data rate and coverage probability of RIS-assisted communications are explicitly derived. Next, performance of large-scale RIS planning is developed in Section IV. Simulation and numerical results are discussed in Section V and, finally, Section VI concludes the paper.

II. SYSTEM MODEL

We consider a two-dimensional RIS, composed of N tunable reflective elements, which is transmitting data to a single antenna user by reflecting an incident RF wave from a single antenna base station (BS). The RIS can dynamically adjust the phase shift induced by each reflecting element. Besides, we assume that the direct links from the BS to the user is blocked by obstacles, such as buildings. Such assumption is highly applicable in indoor communication scenarios. Moreover, there are several works that study outdoor RIS-assisted communication systems under a blocked direct link [2]- [11]. This assumption is likely to be true for 5G and beyond mmWave and sub-mmWave communication systems, which are known to suffer from high path and penetration losses resulting in signal blockages [13]. Assuming transmission over flat-fading channels, the resulting overall channel gain is given by

$$h = \sqrt{\rho_L} \mathbf{g} \Phi \mathbf{h}^H, \quad (1)$$

where ρ_L is the average SNR of the RIS-assisted link, $\mathbf{g} = [g_1, \dots, g_N] \in \mathbb{C}^{1 \times N}$ is the fading channel coefficients between the BS and the RIS, $\mathbf{h} = [h_1, \dots, h_N] \in \mathbb{C}^{1 \times N}$ denotes the channel vector between the RIS and the user. In addition, $\Phi = \text{diag}(e^{j\phi_1}, e^{j\phi_2}, \dots, e^{j\phi_N}) \in \mathbb{C}^{N \times N}$ accounts for the effective phase shifts applied by all RIS reflecting elements, where $\phi_n \in [0, 2\pi)$, $n = 1, 2, \dots, N$ are the phase-shift variables that can be optimized by the RIS.

In this paper, a general type of distribution is assumed for g_i and h_i , $i = 1, \dots, N$, as specified below.

Assumption 1: We assume that $|h_i|$ and $|g_i|$ are independent and non identically distributed (i.n.i.d) Fox's H-distributed RVs with respective pdf

$$f_{|y|_i}(x) = \kappa_i^y H_{p_i^y, q_i^y}^{m_i^y, n_i^y} \left(c_i^y x \left| \begin{array}{l} (a_{ij}, A_{ij})_{j=1:p_i^y}^y \\ (b_{ij}, B_{ij})_{j=1:q_i^y}^y \end{array} \right. \right), \quad (2)$$

where $y \in \{h, g\}$, and $H[\cdot]$ stands for the Fox'H function [20, Eq. (1.2)]. The Fox's \mathcal{H} function pdf considers homogeneous radio propagation conditions and captures composite effects of multipath fading and shadowing, subsuming large variety of extremely important or generalized fading distributions used in wireless communications such as Rayleigh, Nakagami-m, Weibull α - μ , (generalized) \mathcal{K} -fading, the Fisher-Snedecor \mathcal{F} , and EGK, as shown in [16] and references therein. Furthermore, the Fox's \mathcal{H} -function distribution provides enough

flexibility to account for disparate signal propagation mechanisms and well-fitted to measurement data collected in diverse propagation environments having different parameters.

III. RIS PERFORMANCE IN GENERALIZED FADING

Using H-transforms, we now establish a unifying framework to analyze fundamental performances for RIS-assisted wireless communication where the fading envelope is described by Fox's H distribution. The performance metrics are the outage probability and channel capacity, as well as their tradeoffs such as diversity gain.

A. Outage Probability

Lemma 1: For a given SNR threshold ρ , the outage probability in RIS-supported network is

$$\begin{aligned} \bar{\Pi}(\rho, N) &= \max_{\phi_1, \dots, \phi_n} \text{P}(\log_2(1 + \rho_L |\mathbf{g} \Phi \mathbf{h}^H|^2) < \rho) \\ &= \text{P}\left(\log_2\left(1 + \rho_L \left(\sum_{i=1}^N |h_i| |g_i|\right)^2\right) < \rho\right) \end{aligned} \quad (3)$$

Proof: For any given Φ , the coverage expression in (3) is achieved from the capacity of an additive white Gaussian noise channel, where $\mathbf{g} \Phi \mathbf{h}^H = \sum_{i=1}^N h_i g_i e^{-j\phi_n}$. The maximum coverage is achieved when the phase-shifts are selected as $\phi_n = -\arg(h_n + g_n)$, $n = 1, \dots, N$.

Proposition 1: The outage probability achieved by RIS-assisted communication is

$$\begin{aligned} \bar{\Pi}(\rho, N) &= \tau H_{0,1:\tilde{p}_1, \tilde{q}_1, \dots, \tilde{p}_N, \tilde{q}_N}^{0,0:\tilde{m}_1, \tilde{n}_1, \dots, \tilde{m}_N, \tilde{n}_N} \\ &\left[\begin{array}{l} \tilde{c}_1 \sqrt{\rho_t} \\ \vdots \\ \tilde{c}_N \sqrt{\rho_t} \end{array} \middle| - : (1, 1), (\delta_1, \Delta_1)_{\tilde{p}_1}; \dots; (1, 1), (\delta_N, \Delta_N)_{\tilde{p}_N} \right] \\ &\quad (0; 1, \dots, 1) : (\xi_1, \Xi_1)_{\tilde{q}_1}; \dots; (\xi_N, \Xi_N)_{\tilde{q}_N} \end{aligned} \quad (4)$$

where $\rho_t = \frac{2\rho-1}{\tau}$, $\tau = \prod_{i=1}^N \frac{\kappa_i^h \kappa_i^g}{c_i^h c_i^g}$, $\tilde{c}_i = c_i^h c_i^g$ and $H[\cdot, \dots, \cdot]$ is the multivariable Fox'H-function whose definition in terms of multiple MellinBarnes type contour integral is given in [20, Definition A.1] where

$$(\delta_i, \Delta_i)_{\tilde{p}_i} = \left((a_{ij} + A_{ij}, A_{ij})_{j=1:p_i^h}^h, (a_{ij} + A_{ij}, A_{ij})_{j=1:p_i^g}^g \right) \quad (5)$$

$$(\xi_i, \Xi_i)_{\tilde{q}_i} = \left((b_{ij} + B_{ij}, B_{ij})_{j=1:q_i^h}^h, (b_{ij} + B_{ij}, B_{ij})_{j=1:q_i^g}^g \right) \quad (6)$$

Moreover, $\tilde{m}_i = m_i^h + m_i^g$, $\tilde{n}_i = n_i^h + n_i^g + 1$, $\tilde{q}_i = q_i^h + q_i^g$, and $\tilde{p}_i = p_i^h + p_i^g + 1$.

Proof: The probability in (4) is obtained by defining the random variables $\mathcal{S} = \sum_{i=1}^N |h_i| |g_i|$ and recognizing that

$$\bar{\Pi}(\rho, N) = \frac{1}{2\pi j} \int_{\mathcal{L}} s^{-1} \Psi_{\mathcal{S}}(s) e^{s\sqrt{\rho_t}} ds, \quad (7)$$

where $\Psi_{\mathcal{S}}(s) = \prod_{i=1}^N \mathcal{L}(f_{|h_i||g_i|})(s)$ where $\mathcal{L}(\cdot)$ stands for the Laplace transform. After an appropriate parameter setting in the product of two Fox' H functions using [24, Theorem (4.1)] then their Laplace transform by applying [20, Eq. (2.20)], $\Psi_{\mathcal{S}}$ follows as shown in (8) at the top of the next page. By plugging (8) into (7), the outage probability can be written

$$\Psi_S(s) = \frac{\tau}{(2\pi w)^r} \int_{\mathcal{L}_1} \cdots \int_{\mathcal{L}_N} \prod_{i=1}^N \left(\frac{\Gamma(-u_i) \Theta_i(u_i)}{\tilde{c}_i^{u_i}} \right) s^{\sum_{i=1}^N u_i} du_1 du_2 \dots du_N$$

$$\text{where } \Theta_j(u_j) = \frac{\prod_{j=1}^{\tilde{m}_j} \Gamma(\xi_j + \Xi_j u_j) \prod_{j=1}^{\tilde{p}_j} \Gamma(1 - \delta_j - \Delta_j u_j)}{\prod_{j=\tilde{n}_j+1}^{\tilde{p}_j} \Gamma(\delta_j + \Delta_j u_j) \prod_{j=\tilde{m}_j+1}^{\tilde{q}_j} \Gamma(1 - \xi_j - \Xi_j u_j)}. \quad (8)$$

$$\begin{aligned} \frac{1}{2\pi j} \int_{\mathcal{L}} s^{-1} \Psi_S(s) e^{sz} ds &= \frac{\tau}{(2\pi w)^N} \int_{\mathcal{L}_1} \cdots \int_{\mathcal{L}_N} \prod_{i=1}^N \left(\frac{\Gamma(-u_i) \Theta_i(u_i)}{\tilde{c}_i^{u_i}} \right) \\ &\quad \times \frac{1}{2\pi j} \int_{\gamma+w\infty}^{\gamma-w\infty} e^{sz} s^{\sum_{i=1}^N u_i - 1} ds du_1 du_2 \dots du_N \\ &= \frac{\tau}{(2\pi w)^N} \int_{\mathcal{L}_1} \cdots \int_{\mathcal{L}_N} \prod_{i=1}^N \left(\frac{\Gamma(-u_i) \Theta_i(u_i)}{\tilde{c}_i^{u_i}} \right) \frac{z^{-\sum_{i=1}^N u_i}}{\Gamma(1 - \sum_{i=1}^N u_i)} du_1 du_2 \dots du_N. \end{aligned} \quad (9)$$

as in (9), where recalling that $\frac{1}{2\pi j} \int_{\mathcal{L}} s^{-a} e^{sz} ds = \frac{z^{a-1}}{\Gamma(a)}$ and harnessing on the multiple Mellin-Barnes type contour integral of the multivariate Fox'H function [20, Definition A.1], yield the desired result after some manipulations.

Remark 1: When $N = 1$, the outage probability reduces to

$$\begin{aligned} \bar{\Pi}(\rho, 1) &= \tau \mathcal{H}_{\tilde{p}_1, \tilde{q}_1+1}^{\tilde{m}_1, \tilde{n}_1} \left[\tilde{c}_1 \sqrt{\rho t} \left| \begin{array}{c} (1, 1), (\delta_1, \Delta_1)_{\tilde{p}_1} \\ (\xi_1, \Xi_1)_{\tilde{q}_1}, (0, 1) \end{array} \right. \right] \\ &\stackrel{(a)}{=} 1 - \kappa^h \kappa^g \sqrt{\rho t} \\ &\quad \times \mathcal{H}_{\tilde{p}^h + \tilde{p}^g + 1, \tilde{q}^h + \tilde{q}^g + 1}^{m^h + m^g + 1, n^h + n^g} \left[c^h c^g \sqrt{\rho t} \left| \begin{array}{c} (\delta - \Delta, \Delta)_{\tilde{p}^h + \tilde{p}^g}, (0, 1) \\ (-1, 1), (\xi - \Xi, \Xi)_{\tilde{q}^h + \tilde{q}^g} \end{array} \right. \right] \end{aligned} \quad (10)$$

where (a) follows from applying [24, Eq. (3.8)].

So far, driven by the common observation that the general case with respect to N and fading distribution is rather untractable [2]- [21], previous works settled for only the special case when $N = 1$ and Rayleigh fading. In this case, the outage probability is obtained in [21, Eq. (15)]. In this paper, the special case $N = 1$ specialises from the general formulas in (10). Moreover, in the special case of Rayleigh fading (i.e., when $\tilde{m} = 2$, $\tilde{n} = 0$, $\tilde{p} = 1$, $\tilde{q} = 2$, $\tau = 1$, $(b, B)^h = (b, B)^g = (\frac{1}{2}, \frac{1}{2})$) and after resorting to [24, Eq. (2.45)] and [24, Eq. (2.47)], (10) reduces to

$$\bar{\Pi}(\rho, 1) = 1 - \sqrt{\rho t} \mathcal{H}_{0,2}^{2,0} \left[\sqrt{\rho t} \left| \begin{array}{c} - \\ (-\frac{1}{2}, 1), (\frac{1}{2}, 1) \end{array} \right. \right], \quad (11)$$

which coincides with [21, Eq. (15)] where the Fox's H function in (11) represents the Bessel function of the second kind and first order [20, Eq. (1.128)].

Moreover, based on harmonic-geometric means inequality [28, Sec. 11.116], the outage probability is bounded by

$$\begin{aligned} \bar{\Pi}(\rho, N) &\geq \bar{\Pi}_{LB}(\rho, N) = \mathbb{P} \left(\prod_{i=1}^N |h_i| |g_i| < \left(\frac{\sqrt{\rho t}}{N} \right)^N \right) \\ &= \frac{1}{2\pi j} \int_{\mathcal{L}} s^{-1} \mathcal{L}(\mathcal{f}_{\prod_{i=1}^N |h_i| |g_i|})(s) e^{s \left(\frac{\sqrt{\rho t}}{N} \right)^N} ds. \end{aligned} \quad (12)$$

By an appropriate parameter setting in the product of N Fox' H function using [24, Theorem (4.1)] and applying [20, Eq. (2.20)] and [20, Eq. (2.21)] for the Laplace transform and its

inverse, we obtain the outage probability lower bound as given by

$$\bar{\Pi}_{LB}(\rho, N) = \tau \mathbb{H}_{\sum_{i=1}^N \tilde{p}_i + 1, \sum_{i=1}^N \tilde{q}_i + 1}^{\sum_{i=1}^N \tilde{m}_i, \sum_{i=1}^N \tilde{n}_i + 1} \left[\left(\frac{\sqrt{\rho t}}{N} \right)^N \prod_{i=1}^N \tilde{c}_i \left| \begin{array}{c} (1, 1), (\delta_j, \Delta_j)_{\tilde{p}_j, j=1:N} \\ (\xi_j, \Xi_j)_{\tilde{q}_j, j=1:N}, (0, 1) \end{array} \right. \right], \quad (13)$$

where $\hat{n}_i = n_i^h + n_i^g$ and $\hat{p}_i = p_i^h + p_i^g$. Note that, by virtue of harmonic-geometric means inequality, the multivariate Fox'H representation of the outage portability in (4) culminate in a Fox' H function of a single variable.

Corollary 1: When $|h_i|$ and $|g_i|$ are i.i.d. Fox's H-distributed RVs, $\bar{\Pi}_{LB}(\rho, N)$ becomes

$$\begin{aligned} \bar{\Pi}_{LB}(\rho, N) &= \left(\frac{\kappa}{c} \right)^{2N} \mathbb{H}_{2Np+1, 2Nq+1}^{2Nm, 2Nn+1} \\ &\left[\left(\frac{\sqrt{\rho t}}{N} \right)^N c^{2N} \left| \begin{array}{c} (1, 1), \{(\delta, \Delta)\}_{1:Np} \\ \{(\xi, \Xi)\}_{1:Nm}, (0, 1), \{(\xi, \Xi)\}_{Nm+1:Nq} \end{array} \right. \right] \end{aligned} \quad (14)$$

Proof: The result follows from (14) by letting all Fox's H fading distribution parameters pertaining to $|h_i|$ and $|g_i|$ equal in (2).

Remark 2: The main merit of these outage probability representations is that they rely on a versatile and generic form of the fading distribution while accurately reflecting the behavior of RIS networks in all operating regimes. The derived analytical expressions for the outage probabilities in (4), and (29) are highly generic and novel and can be easily mapped into most existing fading models. Table I lists some commonly-used channel fading distributions and the corresponding expression for $\bar{\Pi}(\rho, N)$. This result is the first in the literature as it represents the exact SNR distribution in RIS-assisted communications in terms of the multivariate Fox's H-function. This is in contrast with the recently reported expressions in [2, Eqs. (4), (7)], [11, Eqs. (3),(9)] and [21, Eq. (17)], who resorted to approximations (CLT in [?] and moment-based Gamma approximation in [21]) to circumvent the intricacy of the exact statistical modeling of RIS-enabled communications. In this paper, the derived analytical

TABLE I
OUTAGE PROBABILITY OF RIS-ASSISTED COMMUNICATIONS OVER WELL-KNOWN FADING CHANNEL MODELS

Instantaneous Fading Distribution	Outage Probability $\bar{\Pi}(\rho, N)$
<p>Nakagami-m Fading [16, Table IV]:</p> $f_{ y _i}(x) = \frac{\sqrt{m_i^y}}{\Gamma(m_i^y)} \mathcal{H}_{0,1}^{1,0} \left[\sqrt{m_i^y} x \mid (m_i^y - \frac{1}{2}, \frac{1}{2}) \right]$	$\bar{\Pi}(\rho, N) = \left(\prod_{i=1}^N \left(\Gamma(m_i^h) \Gamma(m_i^g) \right) \right)^{-1}$ $\mathbb{H}_{0,1:1,2,\dots,1,2}^{0,0:2,1,\dots,2,1} \left[\begin{array}{c} \sqrt{m_1^h m_1^g} \sqrt{\rho t} \\ \vdots \\ \sqrt{m_N^h m_N^g} \sqrt{\rho t} \end{array} \mid \begin{array}{c} - : (1, 1), -; \dots; (1, 1), - \\ (0; 1, \dots, 1) : \{\xi_1, \Xi_1\}; \dots; \{\xi_N, \Xi_N\} \end{array} \right]$ $\{\xi_i, \Xi_i\} = (m_i^h, \frac{1}{2}), (m_i^g, \frac{1}{2})$
<p>α-μ Fading [16, Table IV]:</p> $f_{ y _i}(x) = \frac{\sqrt{\eta_i^y}}{\Gamma(\mu_i^y)} \mathcal{H}_{0,1}^{1,0} \left[\sqrt{\eta_i^y} x \mid (\mu_i^y - \frac{1}{\alpha_i^y}, \frac{1}{\alpha_i^y}) \right]$ <p>where $\eta_i^y = \frac{\Gamma(\mu_i^y + \frac{2}{\alpha_i^y})}{\Gamma(\mu_i^y)}$</p>	$\bar{\Pi}(\rho, N) = \left(\prod_{i=1}^N \left(\Gamma(\mu_i^h) \Gamma(\mu_i^g) \right) \right)^{-1}$ $\mathbb{H}_{0,1:1,2,\dots,1,2}^{0,0:2,1,\dots,2,1} \left[\begin{array}{c} \sqrt{\eta_1^h \eta_1^g} \sqrt{\rho t} \\ \vdots \\ \sqrt{\eta_N^h \eta_N^g} \sqrt{\rho t} \end{array} \mid \begin{array}{c} - : (1, 1), -; \dots; (1, 1), - \\ (0; 1, \dots, 1) : \{\xi_1, \Xi_1\}; \dots; \{\xi_N, \Xi_N\} \end{array} \right]$ $\{\xi_i, \Xi_i\} = (\mu_i^h, \frac{1}{\alpha_i^h}), (\mu_i^g, \frac{1}{\alpha_i^g})$
<p>Fisher-Snedecor \mathcal{F} [15, Eq.(3)]:</p> $f_{ y _i}(x) = \frac{m_i^y}{m_{s_i}^y \Gamma(m_{s_i}^y) \Gamma(m_i^y)} \times \mathcal{H}_{1,1}^{1,1} \left[\frac{m_i^y x}{m_{s_i}^y} \mid \begin{array}{c} (-m_{s_i}^y + \frac{1}{2}, \frac{1}{2}) \\ (m_i^y - \frac{1}{2}, \frac{1}{2}) \end{array} \right]$	$\bar{\Pi}(\rho, N) = \left(\prod_{i=1}^N \left(\Gamma(m_{s_i}^g) \Gamma(m_i^g) \Gamma(m_{s_i}^h) \Gamma(m_i^h) \right) \right)^{-1}$ $\mathbb{H}_{0,1:3,2,\dots,3,2}^{0,0:2,3,\dots,2,3} \left[\begin{array}{c} \sqrt{\frac{m_i^h m_i^g}{m_{s_i}^h m_{s_i}^g}} \sqrt{\rho t} \\ \vdots \\ \sqrt{\frac{m_N^h m_N^g}{m_{s_N}^h m_{s_N}^g}} \sqrt{\rho t} \end{array} \mid \begin{array}{c} - : (1, 1), \{\delta_1, \Delta_1\}; \dots; (1, 1), \{\delta_N, \Delta_N\} \\ (0; 1, \dots, 1) : \{\xi_1, \Xi_1\}; \dots; \{\xi_N, \Xi_N\} \end{array} \right]$ $\{\delta_i, \Delta_i\} = (1 - m_{s_i}^h, \frac{1}{2}), (1 - m_{s_i}^g, \frac{1}{2})$ $\{\xi_i, \Xi_i\} = (m_i^h, \frac{1}{2}), (m_i^g, \frac{1}{2})$
<p>Generalized \mathcal{K} [16, Table IV]:</p> $f_{ y _i}(x) = \frac{\sqrt{m_i^y k_i^y}}{\Gamma(m_i^y) \Gamma(k_i^y)} \times \mathcal{H}_{0,2}^{2,0} \left[x \sqrt{m_i^y k_i^y} \mid (m_i^y - \frac{1}{2}, \frac{1}{2}), (k_i^y - \frac{1}{2}, \frac{1}{2}) \right]$	$\bar{\Pi}(\rho, N) = \left(\prod_{i=1}^N \left(\Gamma(m_i^h) \Gamma(\kappa_i^h) \Gamma(m_i^g) \Gamma(\kappa_i^g) \right) \right)^{-1}$ $\mathbb{H}_{0,1:1,4,\dots,1,4}^{0,0:4,1,\dots,4,1} \left[\begin{array}{c} \sqrt{m_1^h \kappa_1^h m_1^g \kappa_1^g} \sqrt{\rho t} \\ \vdots \\ \sqrt{m_N^h \kappa_N^h m_N^g \kappa_N^g} \sqrt{\rho t} \end{array} \mid \begin{array}{c} - : (1, 1), -; \dots; (1, 1), - \\ (0; 1, \dots, 1) : (\xi_1, \Xi_1)_{p_{11}}; \dots; (\xi_N, \Xi_N)_{p_N} \end{array} \right]$ $\{\xi_i, \Xi_i\} = (m_i^h, \frac{1}{2}), (m_i^g, \frac{1}{2}), (k_i^h, \frac{1}{2}), (k_i^g, \frac{1}{2})$

expressions for the outage probability are obtained via the evaluation of single and multi-variable Fox's H functions. The latter, have been recently frequently used in the literature and for which efficient implementation codes exist in most popular mathematical software packages [17], [29]. Hence, such expressions can be very rapidly and efficiently computed.

B. Diversity Analysis

In an effort to understand the impact of some key system parameters on the outage probability, we analyze the asymptotic regime at high SNR from which we derive the diversity and coding gains. Asymptotic analysis is particularly useful to this framework since the evaluation of the multivariate Fox's H function may encounter underflow problems when N is large.

Proposition 2: The asymptotic expansion of the outage probability $\bar{\Pi}(\rho, N)$ in (4) for high SNRs can be obtained by computing the residue [26]. Let us consider the residue at the points $\zeta_l = (\zeta_1, \dots, \zeta_N)$, where $\zeta_l = \min_{j=1, \dots, \widetilde{m}_l} \left\{ \frac{\xi_{lj}}{\Xi_{lj}} \right\}$, the asymptotic outage probability¹ is obtained as

$$\bar{\Pi}(\rho, N) \approx \frac{\tau}{\Gamma(1 + \sum_{i=1}^N \zeta_i)} \left(\prod_{i=1}^N \tilde{\Theta}_i(-\zeta_i) \tilde{\mathcal{C}}_i^{\zeta_i} \right) \rho t^{\frac{\sum_{i=1}^N \zeta_i}{2}}, \quad (15)$$

¹It should be stressed here that (15) holds when poles at $\{\zeta_1, \dots, \zeta_N\}$ are simple, i.e. $\Xi_{lj}(\xi_{lj} + k) \neq \Xi_{ti}(\xi_{ti} + k')$, $j = 1, \dots, \widetilde{m}_l$, $l = 0, 1, \dots, N$, $k, k' = 0, 1, \dots, N$ [26], which is particularly verified in i.n.i.d fading.

where $\tilde{\Theta}_j(\zeta_j) = \frac{\prod_{i=1, i \neq j}^{\tilde{m}_j} \Gamma(\xi_i + \Xi_i \zeta_j) \prod_{i=1}^{\tilde{n}_j} \Gamma(1 - \delta_i - \Delta_i \zeta_j)}{\prod_{i=\tilde{n}_j+1}^{\tilde{p}_j} \Gamma(\delta_i + \Delta_i \zeta_j) \prod_{i=\tilde{m}_j+1}^{\tilde{q}_j} \Gamma(1 - \xi_i - \Xi_i \zeta_j)}$.

From (15), the diversity order of the considered RIS-assisted system is given by

$$\mathcal{G}_d = \lim_{\rho_L \rightarrow \infty} \frac{\log \bar{\Pi}(\rho, N)}{\log \rho_L} = \frac{\sum_{i=1}^N \zeta_i}{2}. \quad (16)$$

On the other hand, exploiting the outage probability lower bound in (29), the performance trends of RIS-assisted communications scales as

$$\bar{\Pi}_{LB}(\rho, N) \stackrel{(a)}{\approx} \tau h^* \left(\left(\frac{\sqrt{\rho_t}}{N} \right)^N \prod_{i=1}^N \tilde{c}_i \right)^{\min_{l=1, \dots, \sum_{i=1}^N \tilde{m}_i} \zeta_l}, \quad (17)$$

where (a) follows from applying the asymptotic expansion of the Fox's H function in [20, Eq. (1.94)], where h^* follows from an appropriate parameters setting in [26, Eq. (1.5.8)].

It can be inferred from (17), that the outage probability is inversely proportional to N^2 . In fact, the RIS enables the multi-path signals to be added constructively without introducing additional noise. As proved in (17) and earlier in [7] for Rayleigh fading, the downlink SNR of the RIS achieves, asymptotically, the order of $\mathcal{O}(N^2)$, as N increases to infinity. However, the downlink SNRs of a conventional massive MIMO or MIMO relay system, each of which equipped with N antennas, equally increases with $\mathcal{O}(N)$ as proved in [18]. This result shows that, asymptotically, the performance (in terms of SNR) in RIS systems can be twice as much as conventional array systems, without adding radio resources. Hereafter, we specify the asymptotic performance of RIS-assisted communications in small-scale fading (ex. Nakagami- m) and composite small-scale/shadowing fading (ex. generalised \mathcal{K}) environments.

Corollary 2: The asymptotic outage probability of RIS-assisted communications in Nakagami- m fading is

$$\bar{\Pi}(\rho, N) \approx \tau \mathcal{C} \rho_L^{-\sum_{i=1}^N \min\{m_i^g, m_i^h\}}, \quad (18)$$

where ρ_L stands for the average SNR, $\tau = \left(\prod_{i=1}^N \Gamma(m_i^h) \Gamma(m_i^g) \right)^{-1}$ and $\mathcal{C} = \frac{\prod_{i=1}^N \Gamma(m_i^g - \frac{\zeta_i}{2}) \Gamma(m_i^h - \frac{\zeta_i}{2}) \prod_{i=1}^N (m_i^g m_i^h)^{\min\{m_i^g, m_i^h\}}}{\Gamma(1 + 2 \sum_{i=1}^N \min\{m_i^g, m_i^h\})}$. Moreover, resorting to the asymptotic lower bound in (17), it follows that

$$\bar{\Pi}_{LB}(\rho, N) \approx \tau \bar{\mathcal{C}} \left(\frac{\rho_t}{N^2} \right)^{N \min\{m_1^g, m_1^h, \dots, m_N^g, m_N^h\}}, \quad (19)$$

where $\bar{\mathcal{C}} = \frac{\left(\prod_{i=1}^N (m_i^g m_i^h) \right)^{\min\{m_1^g, m_1^h, \dots, m_N^g, m_N^h\}}}{\prod_{i=1}^N \Gamma(m_i^h) \Gamma(m_i^g)}$.

Corollary 2 stipulates that RIS performance degrades when the propagation environment exhibits poor scattering conditions (smaller m^h and m^g). However, at higher frequencies (mmWave and sub-mmWave), the propagation conditions get harsher since mmWave signals are extremely sensitive to objects, including foliage and human body, resulting in signal blockage. Recently, the authors of [22] studied the generalised \mathcal{K} to provides accurate modeling and characterisation of the simultaneous occurrence of multipath fading and shadowing

in mmWave communications. In RIS context we obtain the following Corollary.

Corollary 3: The asymptotic outage probability of RIS-assisted communications in Generalised \mathcal{K} fading is

$$\bar{\Pi}(\rho, N) \approx \tau \mathcal{C} \rho_L^{-\sum_{i=1}^N \min\{\kappa_i^g, m_i^g, \kappa_i^h, m_i^h\}}, \quad (20)$$

where τ and \mathcal{C} follows under the same rational of (18) while using the fourth line in Table I. Corollary 2 reveals that the diversity gain of RIS-assisted communications in composite multi-path shadowing fading channels is limited to the worst channel condition between multipath fading and shadowing on both BS-RIS and RIS-user links.

Corollary 4 (Outage scaling in i.i.d. Fox's H fading): When $|h_i|$ and $|g_i|$ are i.i.d. Fox's H-distributed RVs, then a power-logarithmic series expansion of the outage probability is given by

$$\bar{\Pi}_{LB}(\rho, N) \stackrel{(a)}{\approx} \mathcal{T} \rho_t^{\frac{N\xi}{2\xi}} \ln(\rho_t^{-1})^{2Nm-1}, \quad (21)$$

where (a) follows from applying [26, Eq. (1.4.18)] with $\mathcal{T} = H^* \left(\frac{\kappa}{c} \right)^{2N} \left(\frac{c^N}{N^2} \right)^{N \frac{\xi}{2\xi}}$, where H^* is given in [26, Eq. (1.4.6)]. The above result shows that high SNR outage of RIS-based communications in i.i.d. fading scales as $\rho_L^{-N \frac{\xi}{2\xi}} \ln(\rho_L)^{2Nm-1}$, where ρ_L is the average transmit SNR. Specifically, under i.i.d. Nakagami- m fading we obtain

$$\bar{\Pi}_{LB}(\rho, N) \approx \mathcal{T} \rho_t^{Nm} \ln(\rho_t^{-1})^{2N-1}, \quad (22)$$

implying that the outage scales as $\rho_L^{-N} \ln(\rho_L)^{2N-1}$ in Rayleigh fading. Previously the authors of [21] revealed that the outage decreases at the rate $\rho_L^{-N} \ln(\rho_L)^N$, which coincides with (22) when $N = 1$.

Remark 3 (A hint on RIS-assisted optical communications): The concept of using RISs in free space optical (FSO) links is viable as to relax the line of-sight requirement of FSO systems. Lately, in [23], the concept of using RISs in FSO links was presented as a cost-effective solution for backhauling of cellular systems. However, the focus of [23] was on network planning and the impact of RISs on the FSO channel model was not studied. Recently, the authors of [15], [19] proposed the Fischer-Snedecor \mathcal{F} -distribution, for which the RIS framework is obtained in Table I, for modeling turbulence-induced fading in free-space optical systems. In [15], [19] the small-scale irradiance variations of the propagating wave are modeled by a gamma distribution, while the large-scale irradiance fluctuations follow an inverse gamma distribution. For this new turbulence distribution, the small- and large-scale irradiance variances and henceforth m and m_s in [line 3, Table I] are expressed in terms of important parameters affecting optical propagation, including the atmospheric refractive-index structure parameter, the propagation path length, the inner and the outer scale of turbulence as shown in [19, Eqs. (13),(14), (16), (17)].

Remark 4: Corollary 2,3, and 4 demonstrate the unification of various FSO turbulent and RF fading scenarios into a single closed-form expression for RISs performance. More importantly, capitalizing on the versatility of the Fox's H distribution and the generality of the Fox's H transform theory, the framework of this paper provides a powerful baseline

$$\begin{aligned}
\mathcal{E}(\rho_L, N) &= \frac{\tau}{\ln(2)(2\pi w)^r} \int_{\mathcal{L}_1} \cdots \int_{\mathcal{L}_N} \frac{\prod_{i=1}^N \left(\frac{\Gamma(-u_i)\Theta_i(u_i)}{\tilde{c}_i^{u_i}} \right)}{\Gamma(1 - \sum_{i=1}^N u_i)} \int_0^\infty E_i(-s) \int_0^\infty z^{1-\sum_{i=1}^N u_i} e^{-\rho_L s z^2} dz ds du_1 du_2 \dots du_N \\
&= \frac{\tau}{\ln(2)(2\pi w)^r} \int_{\mathcal{L}_1} \cdots \int_{\mathcal{L}_N} \frac{\prod_{i=1}^N \left(\frac{\Gamma(-u_i)\Theta_i(u_i)}{(\rho_L \tilde{c}_i)^{u_i}} \right)}{\Gamma(1 - \sum_{i=1}^N u_i)} \frac{\Gamma\left(\frac{\sum_{i=1}^N u_i}{2}\right)}{\Gamma\left(1 - \frac{\sum_{i=1}^N u_i}{2}\right)} du_1 du_2 \dots du_N. \tag{24}
\end{aligned}$$

$$\mathcal{E}(\rho_L, N) = \frac{\tau}{\ln(2)} \text{H}_{2,1:\tilde{p}_1, \tilde{q}_1, \dots, \tilde{p}_N, \tilde{q}_N}^{0,1:\tilde{m}_1, \tilde{n}_1, \dots, \tilde{m}_N, \tilde{n}_N} \left[\begin{array}{c} \rho_L \tilde{c}_1 \\ \vdots \\ \rho_L \tilde{c}_N \end{array} \middle| \begin{array}{l} (1; -\frac{1}{2}, \dots, -\frac{1}{2}), (1; -\frac{1}{2}, \dots, -\frac{1}{2}) : (1, 1), (\delta_1, \Delta_1)_{\tilde{p}_1}; \dots; (1, 1), (\delta_N, \Delta_N)_{\tilde{p}_N} \\ (1; -1, \dots, -1) : (\xi_1, \Xi_1)_{\tilde{p}_1}; \dots; (\xi_N, \Xi_N)_{\tilde{p}_N} \end{array} \right] \tag{25}$$

model to build upon to potentially extend the results of this paper to many other directions. Without any pretention of being able to discuss them all due to lack of space, the most prominent directions for future works include MIMO and cellular networks relying on RISs. Interestingly, the proposed framework not only promotes general generic fading channels, but also other generalization path-loss models (see Section IV), LOS/NLOS propagation and random blockage.

C. Channel Capacity

Proposition 3: The RIS-assisted communication channel capacity defined as

$$\mathcal{E}(\rho_L, N) \triangleq \frac{E \left\{ \ln \left(1 + \rho_L \left(\sum_{i=1}^N |h_i| |g_i| \right)^2 \right) \right\}}{\ln(2)} \tag{23}$$

is obtained as in (25) at the top of the next page.

Proof: The ergodic capacity can be expressed as

$$\mathcal{E} = \int_0^\infty E_i(-x) \frac{\partial \Psi_{\mathcal{S}^2}(\rho_L x)}{\partial x} dx, \tag{26}$$

where $E_i(\cdot)$ stands for the exponential integral function [28]. Moreover, referring to the relation with the MGF $\Psi_{\mathcal{S}^2}(s)$ and its derivative, i.e. $\frac{\partial \Psi_{\mathcal{S}^2}(s)}{\partial s} = -\mathbb{E}\{\mathcal{S}^2 e^{-s\mathcal{S}^2}\} = -\int_0^\infty x^2 e^{-sx^2} f_{\mathcal{S}}(x) dx$, where $f_{\mathcal{S}}(x)$ is the PDF of \mathcal{S} obtained from differentiating (9). Plugging all together, as shown in (26) at the top of the next page, then applying [28, Eq. (3.478)] and [28, Eq. (6.223)] and recalling the Mellin Barnes integral representation of the multivariable Fox' H function [20, Definition A.1], yields the desired result after several manipulations.

Remark 5: When $N = 1$, then with the aid of (10) and recalling that $\mathcal{E} = \frac{1}{\ln(2)} \int_0^\infty \frac{1 - \bar{\Pi}(x, 1)}{1+x} dx$, the ergodic capacity is expressed as

$$\begin{aligned}
\mathcal{E}(\rho_L, N) &= \frac{\kappa^h \kappa^g}{\ln(2) \sqrt{\rho_L}} \int_0^\infty \sqrt{x} \text{H}_{1,1}^{1,1} \left[x \middle| \begin{array}{l} (0, 1) \\ (0, 1) \end{array} \right] \\
&\quad \text{H}_{\tilde{p}_1, \tilde{q}_1+1}^{\tilde{m}_1+1, \tilde{n}_1-1} \left[\tilde{c}_1 \sqrt{\frac{x}{\rho_L}} \middle| \begin{array}{l} (\delta_1 - \Delta_1, \Delta_1)_{\tilde{p}_1}, (0, 1) \\ (-1, 1), (\xi_1 - \Xi_1, \Xi_1)_{\tilde{q}_1} \end{array} \right] dx \tag{27}
\end{aligned}$$

which after applying [20, Eq. (2.3)] and [20, Eq. (1.60)] yields

$$\begin{aligned}
\mathcal{E}(\rho_L, N) &= \frac{\tau}{\ln(2)} \\
&\quad \text{H}_{\tilde{p}_1+1, \tilde{q}_1+2}^{\tilde{m}_1+2, \tilde{n}_1} \left[\frac{\tilde{c}_1}{\sqrt{\rho_L}} \middle| \begin{array}{l} (0, \frac{1}{2}), (\delta_1, \Delta_1)_{\tilde{p}_1}, (1, 1) \\ (0, 1), (0, \frac{1}{2}), (\xi_1, \Xi_1)_{\tilde{q}_1} \end{array} \right]. \tag{28}
\end{aligned}$$

While the above result reduces to [21, Eq. (24)] in Rayleigh fading, it unifies the performance of single-element RIS-enabled communications in a plethora of fading channels stemming from the versatile Fox's H fading model.

When $N \geq 2$, a lower bound on the ergodic capacity is obtained from (29) after following similar steps as in (28), thereby yielding

$$\begin{aligned}
\mathcal{E}(\rho_L, N) &\geq \frac{\tau}{\ln(2)} \text{H}_{\sum_{i=1}^N \tilde{p}_i+2, \sum_{i=1}^N \tilde{q}_i+2}^{\sum_{i=1}^N \tilde{m}_i+2, \sum_{i=1}^N \tilde{n}_i+1} \\
&\quad \left[\frac{\prod_{i=1}^N \tilde{c}_i}{(N \sqrt{\rho_L})^N} \middle| \begin{array}{l} (0, \frac{N}{2}), (\delta_j, \Delta_j)_{\tilde{p}_j, j=1:N}, (1, 1) \\ (0, 1), (0, \frac{N}{2}), (\xi_j, \Xi_j)_{\tilde{m}_j, j=1:\tilde{q}_j} \end{array} \right]. \tag{29}
\end{aligned}$$

For high SNR, i.e. $\rho_L \gg 1$, and relying on the same rationale leading to Proposition 2, (17) and (22), we show that the ergodic capacity of N elements RIS-assisted communications increases with the rate $\ln(\rho_L)$. This is due to [26, Eq. (1.8.13)] while assuming that $\Xi_{lj}(\xi_{lj} + k) \neq \Xi_{ti}(\xi_{ti} + k')$, $j = 1, \dots, \tilde{m}_l$, $l = 0, 1, \dots, N$, $k, k' = 0, 1, \dots, N$, thereby only the poles of $\Gamma(s)$ and $\Gamma(Ns/2)$ in (29) coincide with order 2.

IV. PERFORMANCE OF LARGE-SCALE RIS DEPLOYMENT

In order to evaluate the efficiency of large scale deployment of RIS, it is curial to select an appropriate model for the path-loss experienced by the received signal through RIS-assisted communications. Recently, the authors of [12] stipulated that the transmitter-RIS-path loss scales as $N^2(d+r)^{-\alpha}$, where d and r are the BS-IRS, and IRS-receiver distances, respectively, and α is the path-loss exponent. In what follows, we consider a homogeneous binomial point process (BPP) [27] Φ , with M transmitting RISs uniformly distributed in a finite disc $b(0, R)$ with radius R . Assuming that each receiver can be connected to its nearest RIS, then the outage probability of a typical receiver located at the origin is given by

$$\bar{\Pi}(\rho, N, M) = \int_0^R \mathcal{L}^{-1} \left\{ \frac{\Psi(s)}{s}, \frac{\sqrt{\rho t}}{(d+x)^{-\frac{\alpha}{2}}} \right\} f_r(x) dx. \tag{30}$$

TABLE II
CHANNEL CAPACITY OF RIS-ASSISTED COMMUNICATIONS OVER WELL-KNOWN FADING CHANNEL MODELS

Instantaneous Fading Distribution	Channel Capacity $\mathcal{E}(\rho_L, N)$
Nakagami- m Fading [16, Table IV]:	$\mathcal{E}(\rho_L, N) = \frac{\left(\prod_{i=1}^N (\Gamma(m_i^h)\Gamma(m_i^g))\right)^{-1}}{\ln(2)}$ $H_{2,1:1,2,\dots,1,2}^{0,1:2,1,\dots,2,1} \left[\begin{array}{c} \sqrt{m_1^h m_1^g \sqrt{\rho t}} \\ \vdots \\ \sqrt{m_N^h m_N^g \sqrt{\rho t}} \end{array} \middle \begin{array}{l} (1; \{-\frac{1}{2}\}_{1:N}, (1; \{-\frac{1}{2}\}_{1:N}) : (1, 1), -; \dots; (1, 1), - \\ (1; 1, \dots, 1) : \{\xi_1, \Xi_1\}; \dots; \{\xi_N, \Xi_N\} \end{array} \right]$ $\{\xi_i, \Xi_i\} = (m_i^h, \frac{1}{2}), (m_i^g, \frac{1}{2})$
α - μ Fading [16, Table IV]:	$\mathcal{E}(\rho_L, N) = \frac{\left(\prod_{i=1}^N (\Gamma(\mu_i^h)\Gamma(\mu_i^g))\right)^{-1}}{\ln(2)}$ $H_{2,1:1,2,\dots,1,2}^{0,1:2,1,\dots,2,1} \left[\begin{array}{c} \sqrt{\eta_1^h \eta_1^g \sqrt{\rho t}} \\ \vdots \\ \sqrt{\eta_N^h \eta_N^g \sqrt{\rho t}} \end{array} \middle \begin{array}{l} (1; \{-\frac{1}{2}\}_{1:N}, (1; \{-\frac{1}{2}\}_{1:N}) : (1, 1), -; \dots; (1, 1), - \\ (1; 1, \dots, 1) : \{\xi_1, \Xi_1\}; \dots; \{\xi_N, \Xi_N\} \end{array} \right]$ $\{\xi_i, \Xi_i\} = (\mu_i^h, \frac{1}{\alpha_i^h}), (\mu_i^g, \frac{1}{\alpha_i^g})$
Fisher-Snedecor \mathcal{F} [15, Eq.(3)]:	$\mathcal{E}(\rho_L, N) = \frac{\left(\prod_{i=1}^N (\Gamma(m_{si}^g)\Gamma(m_{si}^h)\Gamma(m_i^h)\Gamma(m_i^g))\right)^{-1}}{\ln(2)}$ $H_{2,1:3,2,\dots,3,2}^{0,1:2,3,\dots,2,3} \left[\begin{array}{c} \tilde{c}_1 \sqrt{\rho t} \\ \vdots \\ \tilde{c}_N \sqrt{\rho t} \end{array} \middle \begin{array}{l} (1; \{-\frac{1}{2}\}_{1:N}, (1; \{-\frac{1}{2}\}_{1:N}) : (1, 1), \{\delta_1, \Delta_1\}; \dots; (1, 1), \{\delta_N, \Delta_N\} \\ (1; 1, \dots, 1) : \{\xi_1, \Xi_1\}; \dots; \{\xi_N, \Xi_N\} \end{array} \right]$ $\{\delta_i, \Delta_i\} = (1 - m_{si}^h, \frac{1}{2}), (1 - m_{si}^g, \frac{1}{2})$ $\{\xi_i, \Xi_i\} = (m_i^h, \frac{1}{2}), (m_i^g, \frac{1}{2})$
Generalized \mathcal{K} [16, Table IV]:	$\mathcal{E}(\rho_L, N) = \frac{\left(\prod_{i=1}^N (\Gamma(m_i^h)\Gamma(\kappa_i^h)\Gamma(m_i^g)\Gamma(\kappa_i^g))\right)^{-1}}{\ln(2)}$ $H_{2,1:1,4,\dots,1,4}^{0,1:4,1,\dots,4,1} \left[\begin{array}{c} \sqrt{m_1^h \kappa_1^h m_1^g \kappa_1^g \sqrt{\rho t}} \\ \vdots \\ \sqrt{m_N^h \kappa_N^h m_N^g \kappa_N^g \sqrt{\rho t}} \end{array} \middle \begin{array}{l} (1; \{-\frac{1}{2}\}_{1:N}, (1; \{-\frac{1}{2}\}_{1:N}) : (1, 1), -; \dots; (1, 1), - \\ (1; 1, \dots, 1) : (\xi_1, \Xi_1)_{p_{11}}; \dots; (\xi_N, \Xi_N)_{p_{N1}} \end{array} \right]$ $\{\xi_i, \Xi_i\} = (m_i^h, \frac{1}{2}), (m_i^g, \frac{1}{2}), (\kappa_i^h, \frac{1}{2}), (\kappa_i^g, \frac{1}{2})$

where the $f_r(x)$ is the nearest neighbor distance pdf in BPP given by [27]

$$f_r(x) = \frac{2M}{x} \left(1 - \left(\frac{x}{R}\right)^2\right)^{M-1} \left(\frac{x}{R}\right)^2, \quad 0 < x < R. \quad (31)$$

For sake of a tractable solution to (30), we assume that at least one of the transmitters and the receivers is in the surface far-field. While such an assumption is more applicable in indoor communication scenarios with users close to the walls and every wall covered by an IRS (far-field transmitter), Another potential case is to use the IRS as a MIMO transmitter where a single-antenna transmitter near an IRS can be jointly configured to act as a MIMO beamforming array (far-filed receiver). Accordingly, assuming that $d \gg r$, we have $(d+r)^{-\alpha/2} \simeq d^{-\alpha/2} r^{-\alpha/2}$. Then, resorting to (30)

along with the Mellin-Barnes contour integral representation in (9), we obtain the outage probability expression, conditioned on the distance d , as shown at the top of the next page, where $\mathcal{A} = (1, 1), (\delta_1, \Delta_1)_{\tilde{p}_1}; \dots; (1, 1), (\delta_N, \Delta_N)_{\tilde{p}_N}$ and $\mathcal{B} = (\xi_1, \Xi_1)_{\tilde{q}_1}; \dots; (\xi_N, \Xi_N)_{\tilde{q}_N}$.

Proof: From (30) and (9) and applying the binomial expansion [28, Eq. (1.111)] in (31), the outage probability $\bar{\Pi}(\rho, N, M)$ follows from [20, Definition A.1] after some manipulations.

To better understand the trade-off between M and N , a simpler lower bound expression on the outage probability in (32) is obtained from (29) and (31) as

$$\bar{\Pi}_{LB}(\rho, N, M) = M \int_0^1 (1-x)^{M-1} \bar{\Pi}_{LB} \left(\frac{\rho}{(d\sqrt{x})^{-\alpha}}, N \right) dx, \quad (33)$$

$$\bar{\Pi}(\rho, N, M) = 2M\tau \sum_{k=0}^{M-1} \binom{M-1}{k} (-1)^k \mathbb{H}_{0,2;\tilde{p}_1, \tilde{q}_1, \dots, \tilde{p}_N, \tilde{q}_N}^{0,1;\tilde{m}_1, \tilde{n}_1, \dots, \tilde{m}_N, \tilde{n}_N} \left[\begin{array}{c} \tilde{c}_1 R^{\frac{\alpha}{2}} \sqrt{\rho_t} \\ d^{-\frac{\alpha}{2}} \\ \vdots \\ \tilde{c}_N R^{\frac{\alpha}{2}} \sqrt{\rho_t} \\ d^{-\frac{\alpha}{2}} \end{array} \middle| \begin{array}{c} (-1 - 2k; \frac{\alpha}{2}, \dots, \frac{\alpha}{2}) : \mathcal{A} \\ (0; 1, \dots, 1), (-2 - 2k; \frac{\alpha}{2}, \dots, \frac{\alpha}{2}) : \mathcal{B} \end{array} \right], \quad (32)$$

$$\bar{\Pi}_{LB}(\rho, N, M) = \tau \Gamma(M+1) \times \mathbb{H}_{\sum_{i=1}^N \tilde{p}_i + 1, \sum_{i=1}^N \tilde{q}_i + 1}^{\sum_{i=1}^N \tilde{m}_i, \sum_{i=1}^N \tilde{n}_i + 1} \left[\left(\frac{\sqrt{\rho_t}}{(dR)^{-\frac{\alpha}{2}} N} \right)^N \prod_{i=1}^N \tilde{c}_i \middle| \begin{array}{c} (0, N\frac{\alpha}{4}), (1, 1), (\delta_j, \Delta_j) \tilde{p}_j, j=1:N \\ (\xi_j, \Xi_j) \tilde{m}_j, j=1:N, (0, 1), (\xi_j, \Xi_j) \tilde{q}_j, j=1:N, (-M, N\frac{\alpha}{4}) \end{array} \right]. \quad (34)$$

which, applying [20, Eq. (2.53)], evolves to (34) shown at the top of the next page. Similar to (15), the asymptotic outage probability of BPP distributed RIS-assisted networks is obtained by evaluating the residue at the points $\zeta_l = (\zeta_1, \dots, \zeta_N)$, where $\zeta_l = \min_{j=1, \dots, \tilde{m}_l} \left\{ \frac{\xi_{lj}}{\Xi_{lj}} \right\}$, as

$$\bar{\Pi}(\rho, N, M) \approx \frac{\tau \Gamma(M+1) \Gamma\left(1 + \frac{\alpha}{4} \sum_{i=1}^N \zeta_i\right)}{\Gamma\left(1 + \sum_{i=1}^N \zeta_i\right) \Gamma\left(1 + \frac{\alpha}{4} \sum_{i=1}^N \zeta_i + M\right)} \times \left(\prod_{i=1}^N \Theta_i(\zeta_i) \left(\frac{\tilde{c}_i}{(dR)^{-\frac{\alpha}{2}}} \right)^{\zeta_i} \right) \rho_t^{\frac{\sum_{i=1}^N \zeta_i}{2}}. \quad (35)$$

The result in (35) illustrates that the outage probability is a monotonically increasing function of the serving distance d and R (Note that $\zeta_i > 0, i = 1, \dots, N$). Moreover, (35) shows that increasing M provide sustainable performance gain by considerably reducing the outage probability. For a total number of reflecting elements MN , it can be inferred from (35), that increasing N is more beneficial which is mainly due to the prominent SNR gain in (17) which scales with $\mathcal{O}(N^2)$.

V. NUMERICAL RESULTS

In this section, we investigate the performance of the RIS-aided networks and verify our analytical results for the outage probability and ergodic capacity by Monte-Carlo simulation. The multivariate Fox's H-function in all the previously obtained expressions is numerically evaluated using an efficient portable implementation code provided in [17], [29]. Unless otherwise stated, the SNR threshold is set to $\rho = 0$ dB.

Fig. 1 shows the outage probability vs the average transmit SNR for several values of N under Nakagami- m fading with $m_i^g > m_i^h, i = 1, \dots, N$, with $\min_{i=1, \dots, N} \{m_i^h\} = 0.5$. Specifically, the proposed outage exact expression in (4) and its high SNR counterpart in (18) are plotted together with the exact Monte-Carlo simulations. Several observations are gained: i) Our analytical results in (4) exactly match with the simulation results, which confirms the accuracy of our analysis; ii) For different RIS elements count N , we notice that the outage decreases at a rate of ρ_L^{-N} , where ρ_L is the average transmit SNR. This has been analytically proved in (18).

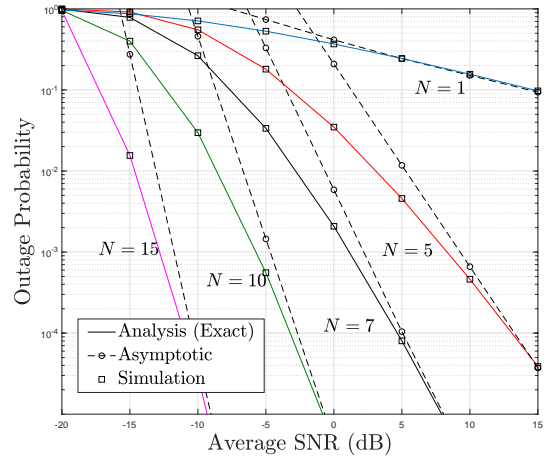


Fig. 1. The outage probability vs the average transmit SNR in Nakagami- m fading.

Fig. 2 shows the outage probability vs the average SNR over α - μ fading evaluated using Table I. For a given N , the outage probability decreases with $\ln(\rho_L)^{2N-1} \rho_L^{-\frac{N\alpha\mu}{2}}$ in i.i.d. α - μ fading which confirms Corollary 2. However in i.n.i.d. α - μ fading the outage probability decreases at a rate of $\rho_L^{-\frac{\min_{i=1, \dots, N} \alpha_i \mu_i}{2}}$ which corroborates (15).

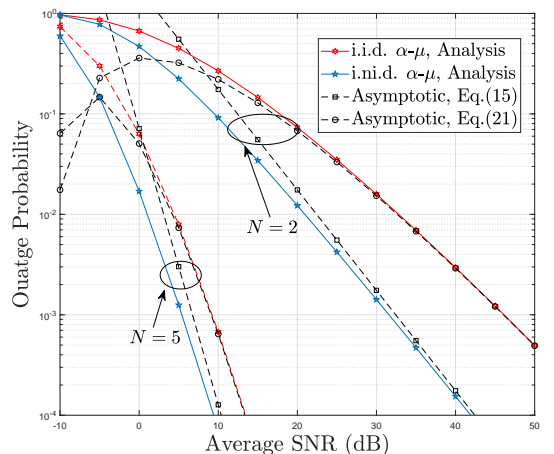


Fig. 2. The outage probability vs the average transmit SNR in α - μ fading.

Fig 3 illustrates the ergodic capacity of RIS-assisted communications over Nakagami- m fading for different reflective RIS elements number N . Importantly, our analytical results in Table II exactly match with the simulation results, which confirms the accuracy of our analysis. Fig. 3 demonstrates that increasing the RIS elements count definitely benefits the ergodic capacity, while the capacity improvement diminishes as the number of elements grows large.

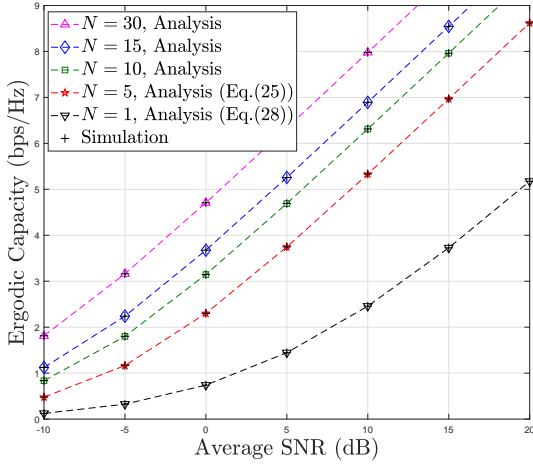


Fig. 3. The average capacity versus the average transmit SNR in Nakagami- m fading.

Fig. 4 depicts the ergodic capacity of a single-element RIS-assisted communication using (28). In the legend, we have identified some particular fading distribution cases that simply stem from the general Fox's H function fading model. The latter, includes as special cases generalized- \mathcal{K} with heavy ($\kappa = 0.5$) and moderate ($\kappa = 1.5$) shadowing, Nakagami- m , Rayleigh ($m = 1$), and α - μ fading models, to name a few (see Table II, [16]). It is worthy to note that such result is totally new and generalises and unifies all previous results pertaining to single-element RIS performance ([21] and references therein).

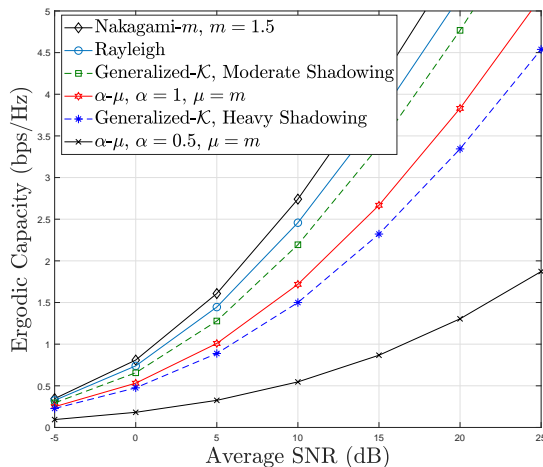


Fig. 4. The average capacity versus the average transmit SNR when $N = 1$.

In fig. 5, we investigate the performance of RIS deployment

using (32) under different number of RISs M and pathloss exponent α . It is observed that both N and M improve the system performance. Yet, interestingly, it is more beneficial to assemble more elements into fewer RISs, in order to maximise the spatial coverage. This phenomenon is also observed for various other choices of R and α . This is mainly due to the prominent SNR gain in (17) which scales with $\mathcal{O}(N^2)$, thus resulting in significant coverage improvement for nearby users, whose performance improvement compensates the generally increased outage area with fewer RISs.

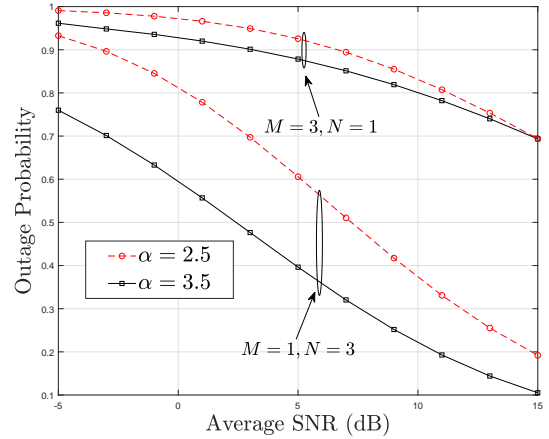


Fig. 5. Spatial outage in Nakagami- m fading with $m = 0.5$ and under different path-loss exponent α and number of RIS M with $MN = 3$ and $R = 50\text{m}$.

VI. CONCLUSION

It has been so far widely admitted that the exact performance of RIS-based communications for arbitrary number of elements N and general fading distribution is rather untractable due to the inherent intricacy of the subject treatment [2]- [21]. In this paper, we have successfully tackled the problem by providing the exact characterisation of outage and ergodic capacity performance of RIS-based communication while remarkably incorporating prominent and generalized fading distributions. Moreover, asymptotic analysis has been conducted for high SNR regime. Our analysis unveils two scaling rates for outage probability both governed by the worst fading multiplied by the RIS elements count N . Capitalizing on the developed statistical framework, we have also characterized the spatial performance of randomly deployed multiple RISs-based communications. We show that there is a great potential to improve the outage performance and thereby the capacity when fewer RISs are deployed each with more reflecting elements. The obtained results could provide helpful guidance for the network deployment and application of RIS technology in future wireless networks.

REFERENCES

- [1] K. B. Letaief, W. Chen, Y. Shi, J. Zhang, and Y. Zhang, "The roadmap to 6G: AI empowered wireless networks," *IEEE Commun. Mag.*, vol. 57, no. 8, pp. 84-90, Aug. 2019.
- [2] E. Basar, M. D. Renzo, J. D. Rosny, M. Debbah, M.-S. Alouini, and R. Zhang, "Wireless communications through reconfigurable intelligent surfaces," *IEEE Access*, vol. 7, pp. 116 753116 773, 2019.

- [3] M. Di Renzo et al., "Smart radio environments empowered by AI reconfigurable meta-surfaces: An idea whose time has come," Mar. 2019. [Online]. Available: <https://arxiv.org/abs/1903.08925>
- [4] C. Huang, A. Zappone, G. C. Alexandropoulos, M. Debbah, and C. Yuen, "Reconfigurable intelligent surfaces for energy efficiency in wireless communication," *IEEE Trans. Wireless Commun.*, vol. 18, no. 8, pp. 41574170, Aug. 2019
- [5] Q.-U.-A. Nadeem, A. Kammoun, A. Chaaban, M. Debbah, and M.-S. Alouini, "Large intelligent surface assisted MIMO communications," arXiv:1903.08127, 2019
- [6] Q. Wu and R. Zhang, "Beamforming optimization for intelligent reflecting surface with discrete phase shifts," arXiv:1810.10718, 201
- [7] Q. Wu and R. Zhang, "Intelligent reflecting surface enhanced wireless network via joint active and passive beamforming," *IEEE Trans. Wireless Commun.*, vol. 18, no. 11, pp. 53945409, Aug. 2019
- [8] M. Cui, G. Zhang, and R. Zhang, "Secure wireless communication via intelligent reflecting surface," May 2019. [Online]. Available: arXiv:1905.10770.
- [9] M. Jung, W. Saad, Y. Jang, G. Kong, and S. Choi, "Reliability analysis of large intelligent surfaces (RISs): Rate distribution and outage probability," arXiv:1903.11456, Mar. 2019. [Online]. Available: <https://arxiv.org/abs/1903.11456v1>
- [10] , "Performance analysis of large intelligent surfaces (RISs): Asymptotic data rate and channel hardening effects," Feb. 2019. [Online]. Available: <https://arxiv.org/abs/1810.05667v2>
- [11] E. Basar, "Transmission Through Large Intelligent Surfaces: A New Frontier in Wireless Communications," in 2019 European Conf. Netw. Commun. (EuCNC), Jun. 2019, pp. 112117.
- [12] K. Ntontin, M. D. Renzo, J. Song, F. Lazarakis, J. de Rosny, D. T. Phan-Huy, O. Simeone, R. Zhang, M. Debbah, G. Lerosey, M. Fink, S. Tretyakov, and S. Shamai, "Reconfigurable intelligent surfaces vs. relaying: Differences, similarities, and performance comparison," available online: <https://arxiv.org/abs/1908.08747>
- [13] M. R. Akdeniz, Yuanpeng Liu, and et. al., "Millimeter wave channel modeling and cellular capacity evaluation," *IEEE J. Sel. Areas Commun.*, vol. 32, no. 6, pp. 1164-1179, June 2014.
- [14] T. Hou, Y. Liu, Z. Song, X. Sun, Y. Chen, and L. Hanzo, "MIMO assisted networks relying on large intelligent surfaces: A stochastic geometry model," 2019. [Online]. Available: <https://arxiv.org/abs/1910.00959>
- [15] K. Yoo, S. Cotton, P. Sofotasios, M. Matthaiou, M. Valkama, and G. Karagiannidis, "The Fisher-SnedecorF distribution: A simple and accurate composite fading model," *IEEE Communications Letters*, no. 99, pp. 11, 2017.
- [16] Y. Jeong, J. W. Chong, H. Shin, and M. Z. Win, "H-Transforms for Wireless Communication," *IEEE Trans. on Inform. Theory*, vol. 61, No. 7, pp. 418433, July 2015
- [17] H. Lei, et al., "Secrecy capacity analysis over α - μ fading channels," *IEEE Commun Let.*, no.99, pp.1-4, Feb. 2017.
- [18] I. Trigui, S. Affes, and A. Stéphenne, "Capacity scaling laws in interference-limited multiple-antenna AF relay networks with user scheduling," *IEEE Trans. Commun.*, vol. 64, no. 8, pp. 3284-3295, Aug. 2016.
- [19] K. P. Alexandropoulos, E. D. X. Evangelos, D. X. Maras, "The Fisher-Snedecor F-distribution Model for Turbulence-Induced Fading in Free-Space Optical Systems", *Journal of Light. Tech.*, Dec. 2019
- [20] A. M. Mathai, R. K. Saxena, and H. J. Haubold, *The H-Function: Theory and Applications*, Springer Science & Business Media, 2009.
- [21] S. Atapattu, R. Fan, P. Dharmawansa, G. Wang, J. Evans, T. A. Tsiftsis, "Reconfigurable Intelligent Surface assisted TwoWay Communications: Performance Analysis and Optimization," available online: <https://arxiv.org/abs/1908.08747>.
- [22] I. Trigui, P. D. Diamantoulakis, S. Affes, G. K. Karagiannidis, "Shadowed FSO/mmWave Systems With Interference", *IEEE Trans. Communications*, vol. 67, no. 9, pp. 6256-6267, 2019.
- [23] Y. Li, N. Pappas, V. Angelakis, M. Piro, and D. Yuan, "Optimization of Free Space Optical Wireless Network for Cellular Backhauling," *IEEE J. Sel. Areas Commun.*, vol. 33, no. 9, pp. 18411854, Sept. 201
- [24] I. Cook, Jr., "The H-function and probability density functions of certain algebraic combinations of independent random variables with H-function probability distribution," DTIC, Fort Belvoir, VA, USA, Tech. Rep. 81-47D, 1981.
- [25] Saxena R.K. On the function of variables Kyungpook Math. J., 17 (1977), pp. 221-226.
- [26] A. Kilbas and M. Saigo, *H-Transforms: Theory and Applications*, CRC Press, 2004.
- [27] S. Srinivasa and M. Haenggi, "Distance distributions in finite uniformly random networks: Theory and applications," *IEEE Trans. Veh. Technol.*, vol. 59, no. 2, pp. 940-949, Feb. 2010
- [28] I. Gradshteyn and I. Ryzhik, *Table of Integrals, Series, and Products*, Academic Press, 1994.
- [29] H. R. Alhennawi, M. M. H. E. Ayadi, M. H. Ismail, and H. A. M. Mourad, "Closed-form exact and asymptotic expressions for the symbol error rate and capacity of the H-function fading channel," *IEEE Transactions on Vehicular Technology*, vol. 65, pp. 1957-1974, Apr. 2016.